

**166th Meeting of the Acoustical Society of America
San Francisco, California
2 - 6 December 2013**

Session 3aPAa: Physical Acoustics

3aPAa1. On the crest factor of noise in full-scale supersonic jet engine measurements

Kent L. Gee*, Tracianne B. Neilsen and Michael M. James

***Corresponding author's address: Physics and Astronomy, Brigham Young University, N283, Provo, UT 84602, kentgee@byu.edu**

An important consideration in characterizing noise from heated, supersonic jets is the crest factor (CF). The large CF in high-speed jet noise is the result of a positively skewed probability density function for the waveform, which translates into infrequently occurring, large-amplitude positive peak pressures. Sufficient system headroom is required in the data acquisition system to provide an accurate representation of these peak pressures and thus avoid clipping or microphone saturation/distortion. But the question remains as to the importance of capturing the single largest pressure out of potentially millions of waveform samples or if a percentile-based CF is adequate. Measurements near a static tactical aircraft reveal CF increases with engine power, with the maximum CF directed upstream of the overall sound pressure level, and a maximum CF of 20 dB at full afterburner. Second, clipping of measured waveforms at different thresholds reveals that a CF definition based on the 99.99 percentile is sufficient to represent overall and band pressure levels to within 0.1 dB and waveform and time-derivative skewnesses to within ~1%. If an estimate of the time-derivative kurtosis is needed within 1% accuracy, then the 99.999 percentile CF is required for headroom estimates.

Published by the Acoustical Society of America through the American Institute of Physics

Background

The vast majority of jet noise literature contains root-mean-square (rms) overall sound pressure levels. However, in data acquisition system design for near-field measurements of high-performance engine noise, it is the peak sound pressure levels that need to be considered. Peak levels in excess of the maximum analog input voltage range, preamplifier limits, or microphone limitations will cause clipping or other distortion of the signal. Thus, a knowledge of the expected crest factor in a jet noise field, in addition to overall level, is important. The crest factor, in decibels, is defined as

$$CF = L_{\text{peak}} - L_{\text{rms}},$$

where L_{peak} is the peak sound pressure level and L_{rms} is the rms overall sound pressure level (OASPL). Although reports of CF are uncommon in the aeroacoustics literature, McInerny¹ calculated crest factors based on time periods of maximum levels in an analysis of several space vehicle launches. In addition to this peak-based definition of crest factor, however, it may make sense to define a percentile-based crest factor, $CF_{\text{XX.XXX}}$, where XX.XXX represents the percentile. This percentile-based definition is likely useful and appropriate because, e.g., one clipped sample in a 30 s long waveform sampled at 96 kHz would have a negligible impact on overall level, spectral shape, or statistics. On the other hand, there is some threshold above which clipping or distortion may impact the measurements noticeably. Examination of changes in calculated measures as a function of clipping severity can therefore be used to determine the appropriateness of a percentile choice.

Presented first in this paper are CF and $CF_{99.999}$. The latter has been chosen because for a 96 kHz sampling rate, this nominally represents one clipped or distorted sample per second. The primary data set used is from the F-35AA Joint Strike Fighter,^{2,3} though briefly considered are corroborative analyses from F-22A Raptor data.⁴ Spatial maps of crest factors over a near-field array are shown as a function of engine condition for a near-field array. The effect of percentile choice on crest factor and, in the case of insufficient data acquisition system headroom, the impact of clipping on the spectrum and statistics are examined.

F-35AA Measurement

The F-35AA static run-up measurements were conducted 18 October, 2008 at Edwards Air Force Base (EAFB), CA. The measurements were made jointly by the Air Force Research Laboratory, Blue Ridge Research and Consulting, and Brigham Young University. A photograph of the tied-down aircraft is displayed in Figure 1.



Figure 1. Tied-down F-35AA aircraft, along with tripods of the near-field microphone array.

Measurements were made using 6.35 mm Type 1 free-field and pressure microphones located at a height of 1.5 m (5 ft). The pressure microphones were oriented skyward, for nominally grazing incidence. The free-field microphones were pointed toward the plume, aimed at a point approximately 6.7 m aft of the aircraft. This point, which is about 7-8 nozzle diameters downstream of the engine exit plane (the same scaled distance used for a previous F-22A experiment^{5,6} in 2004), was set as the origin for defining observation angles. Phased array measurements by Schlinker *et al.*⁷ suggest this was an appropriate choice. During the test, the average wind speed was less than 1 kt and the ambient pressure was virtually constant at 0.914 kPa. Temperature and relative humidity varied from 7 – 16 °C and 21-27%, respectively.

Data acquisition for the array described in this paper was carried out using a National Instruments® 8353 RAID server connected to a PXI chassis containing PXI-4462 cards. Analog input ranges for each channel were adjusted (in 10 dB increments) for low and high-power settings, based on the sensitivity of each microphone, in order to maximize the dynamic range of each of the 24-bit cards. The system sampling frequency was varied between 96 and 204.8 kHz. The lower sampling rate was required because of slower hard drive write speeds for the early-morning tests while the system was cold and during afterburner, where system vibration was greater. The system was located forward of the aircraft and to the sideline (about 70°) at an approximate distance of 35 m. Results are shown for 25% engine thrust request (ETR) through Max afterburner (150% ETR). For Idle through 130% ETR, the waveform length was 30 s. For 150% ETR, the run-up lengths were approximately 10 s.

Results

For each engine condition from 25-150%, L_{rms} , CF, and $\text{CF}_{99,999}$ are shown in sequence.

25%

The results for Idle and 25% are nearly identical, so consequently only 25% is shown. In Figure 2, dots indicate microphone locations, which were primarily determined based on need to assess aircraft maintainer noise exposure. The “x” along the centerline denotes the measurement origin from which angles were calculated. The three radials shown are, moving clockwise, 150, 120, and 90° relative to the engine inlet. A cubic interpolation between measured values was used to produce the maps in

Figure 2. The restriction on placing microphones near the aircraft itself causes those levels to likely be less accurate. At this low engine power, the dominant overall levels are in the forward direction. The peak crest factor, CF, is approximately 13-15 dB and the percentile crest factor, $CF_{99,999}$, is 12.5-13.5 dB. Note that there is more spatial variation in CF, as it represents the single peak value, than in the percentile-based crest factor.

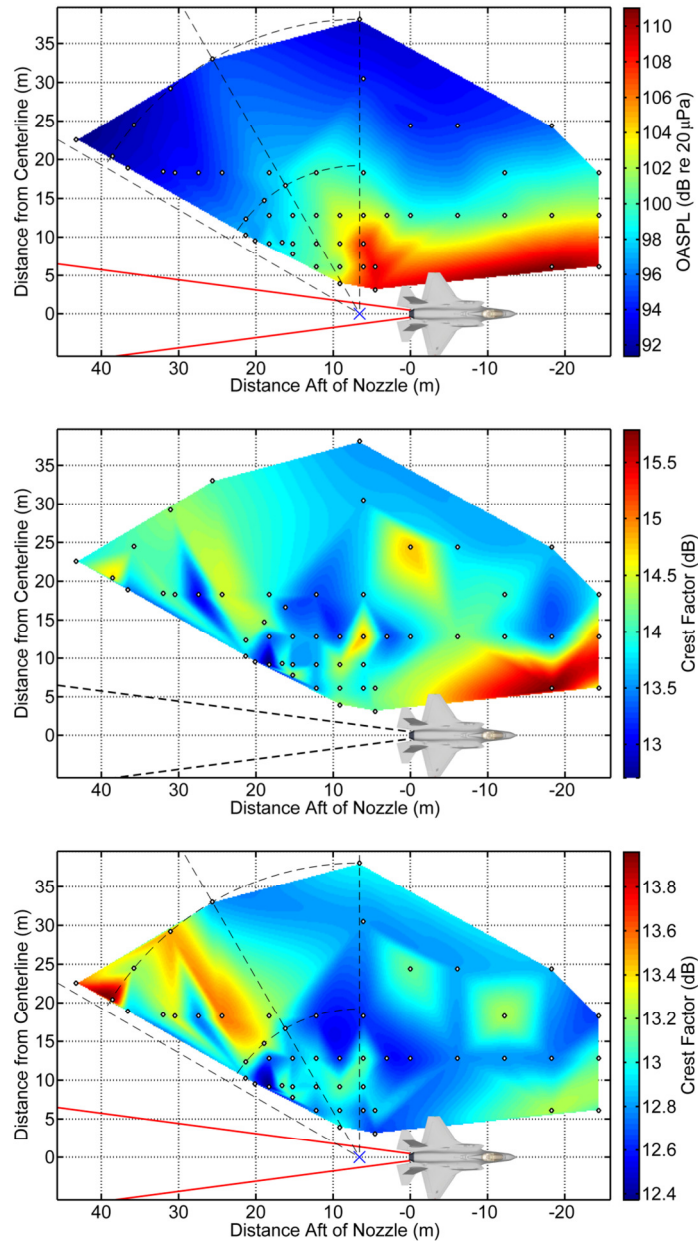


Figure 2. L_{rms} , CF, and $CF_{99,999}$ for 25% ETR.

50%

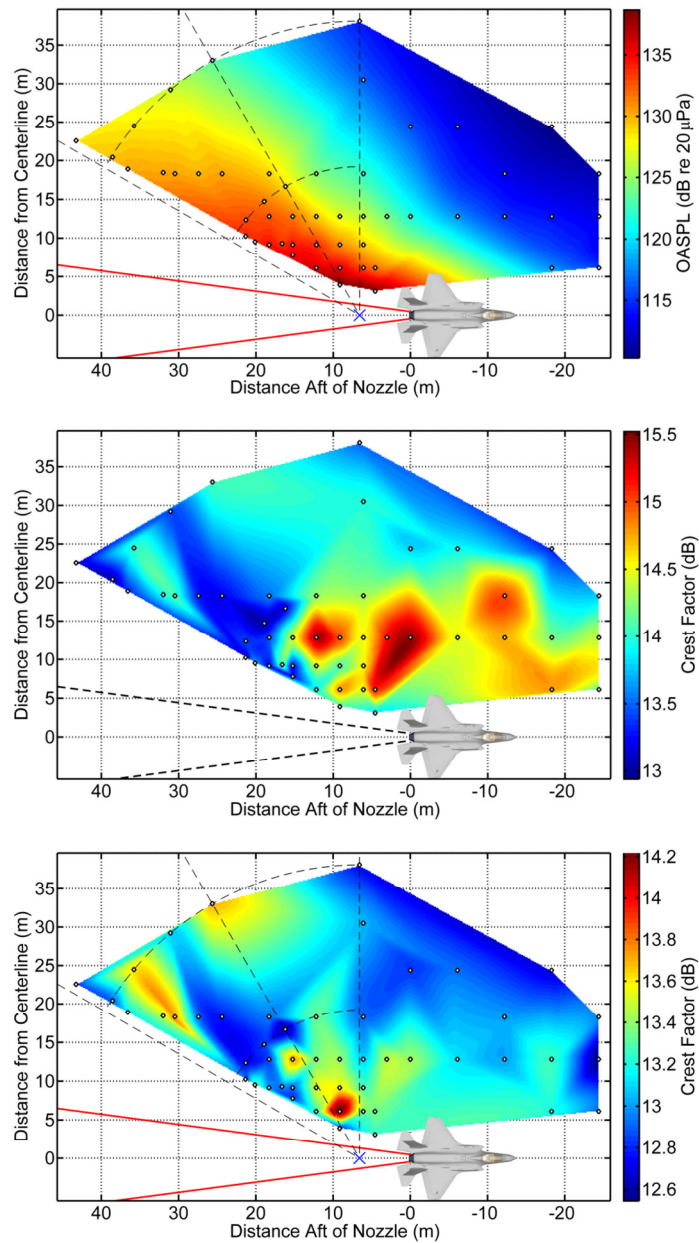


Figure 3. L_{rms} , CF, and $CF_{99,999}$ for 50% ETR.

At 50% ETR in Figure 3, the behavior of the rms sound level changes to be more characteristic of jet mixing noise. However, the crest factor maps have not changed significantly from 25% ETR.

75%

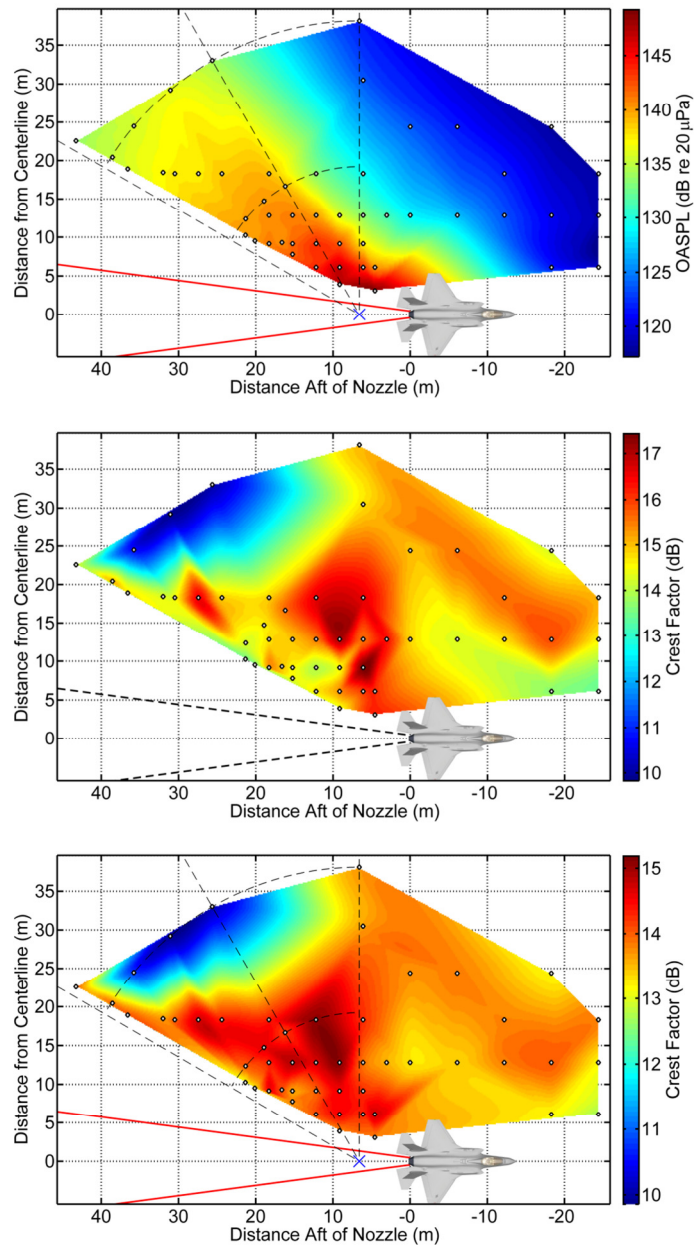


Figure 4. L_{rms} , CF, and $CF_{99,999}$ for 75% ETR.

For 75% ETR in Figure 4, the L_{rms} increases relative to 50% ETR, with a maximum lobe shift of approximately 20° toward the sideline. Excepting the three microphones at 38 m, for which both crest factors are equal to approximately 10 dB, both crest factors have increased significantly from 50% ETR with an average value of ~ 15 dB for CF and ~ 14 dB for $CF_{99,999}$. The cause of the 38 m crest factors being lower is not known, but the fact that it appears at three adjacent microphones suggests its cause is physical.

100%

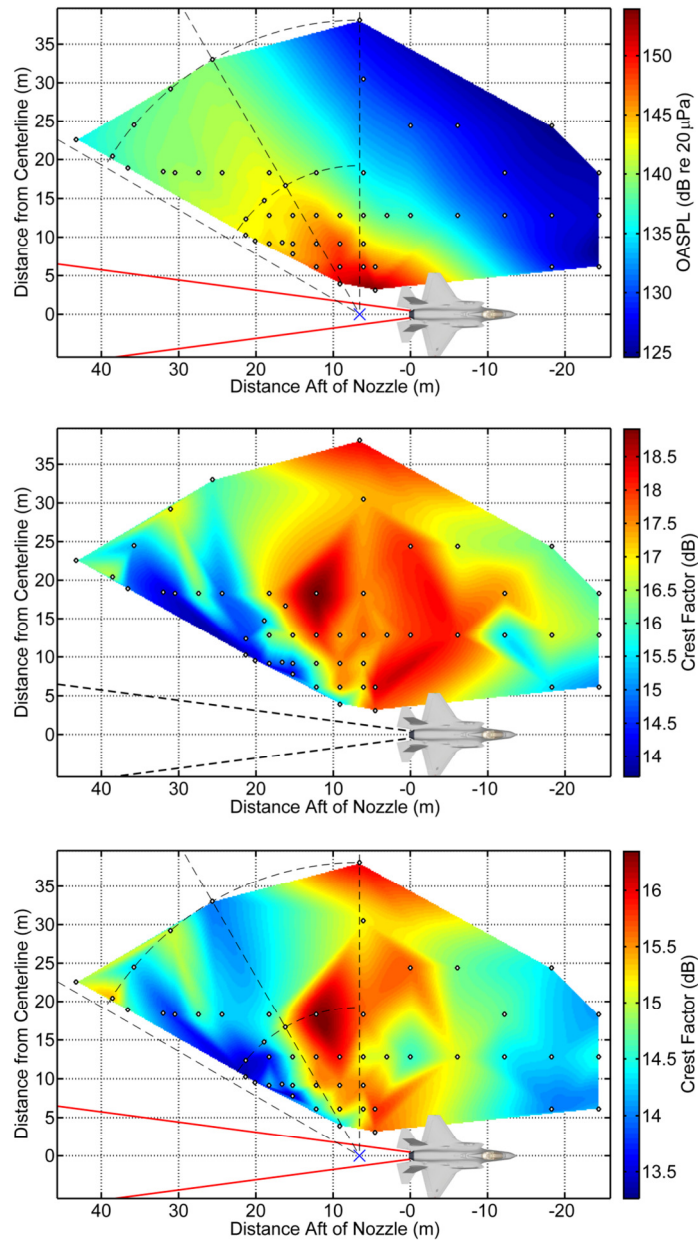


Figure 5. L_{rms} , CF, and $CF_{99,999}$ for 100% ETR (military power).

At military power in Figure 5, the level directivity lobe has shifted upstream an additional $\sim 5^\circ$ from 75%. The crest factors are larger and appear to exhibit a broad lobe centered at the sideline (90°), with $CF_{99,999}$ 2-2.5 dB lower than CF.

130%

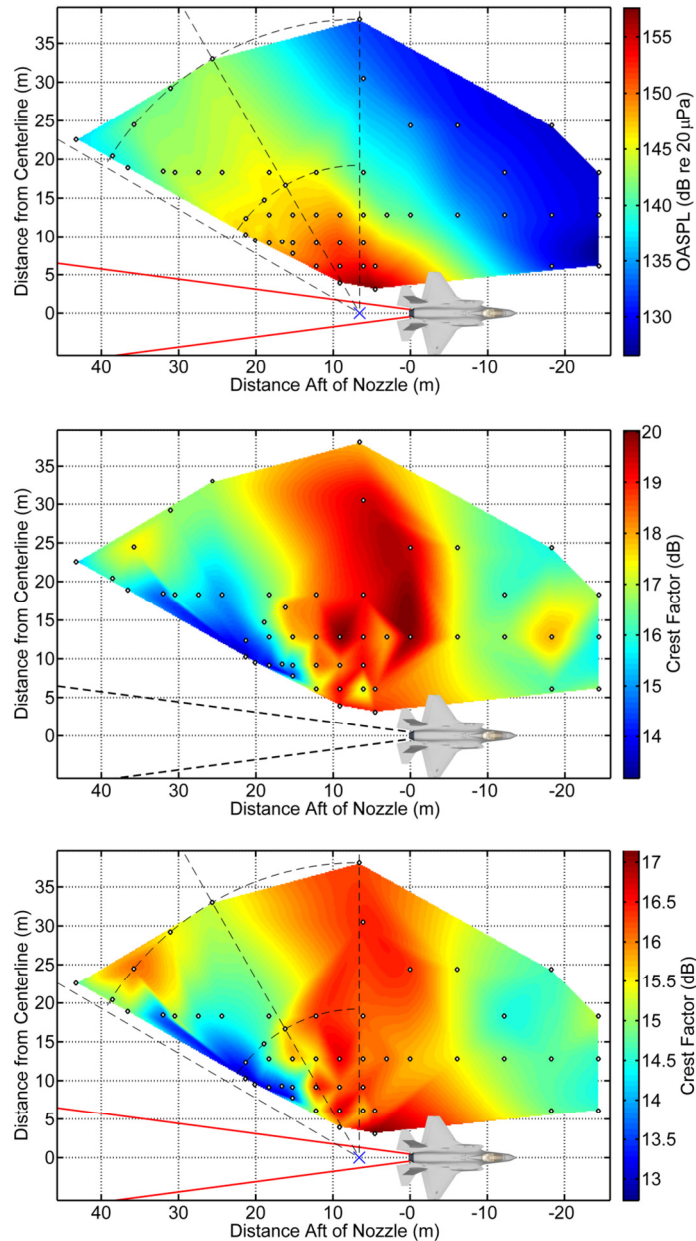


Figure 6. L_{rms} , CF, and $CF_{99,999}$ for 130% ETR.

At 130% afterburner in Figure 6, the maximum CF exceeds 20 dB, but $CF_{99,999}$ has a maximum value of approximately 17 dB. The crest factor lobe upstream of the L_{rms} lobe described for 100% ETR is even more clearly present in this case. The maximum crest factors again appear to peak around 90° , approximately $30\text{--}35^\circ$ upstream of the maximum level. The minimum crest factors occur nearest the shear layer, where the levels are still near the maximum.

150%

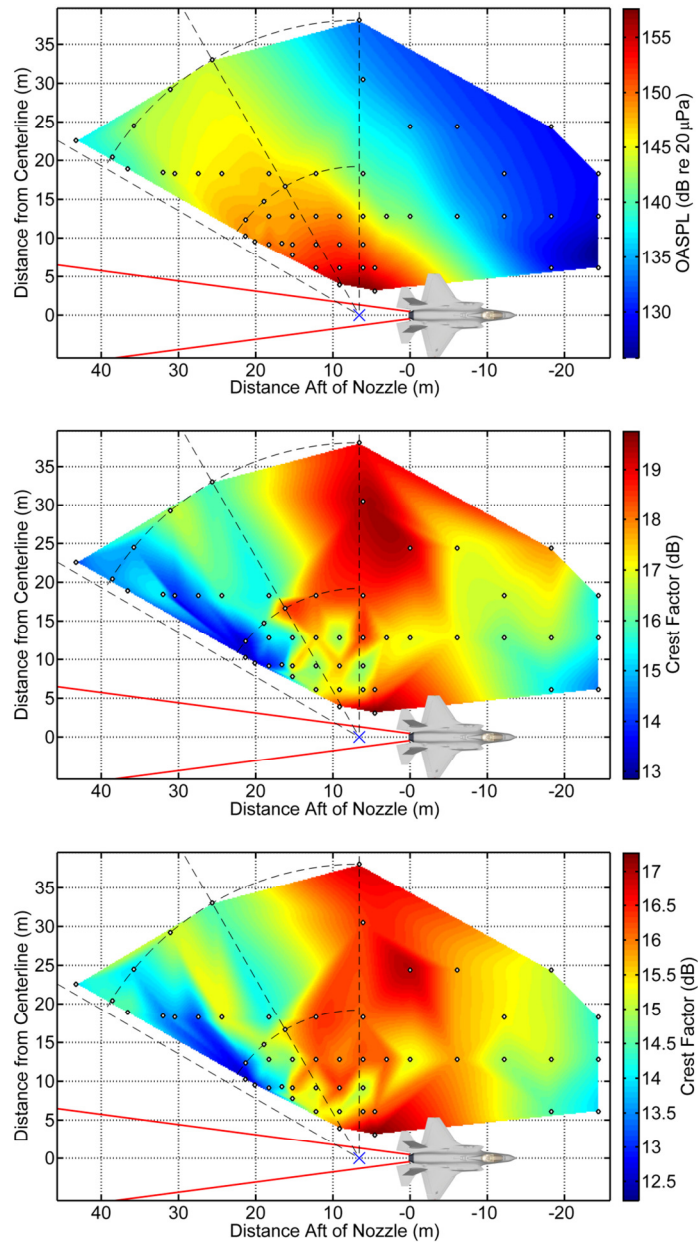


Figure 7. L_{rms} , CF, and $\text{CF}_{99.999}$ for 150% ETR (maximum afterburner).

The behavior for 150% ETR in Figure 7 is similar to the other afterburner in Figure 6, with the peak directivity for crest factor around 90° and minimum along the shear layer, though the maximum CF is about 0.5 dB less than for 130%. However, $\text{CF}_{99.999}$ is slightly greater on average.

Corroborative F-22A Analysis

To perform a basic comparison against the F-35AA data, waveforms from a static experiment on the F-22A at Holloman AFB, July 2009. The 99.999 percentile crest factor at a ground-based array (see Figure 8) was calculated for a single engine at maximum afterburner condition. The data were sampled at 48 kHz and the results were calculated for 10 run-ups. The values in Figure 9 for $CF_{99,999}$ range from mostly 15-17 dB, with lower values downstream (140°). These results appear quantitatively consistent with the F-35AA afterburner measurements for similar locations.

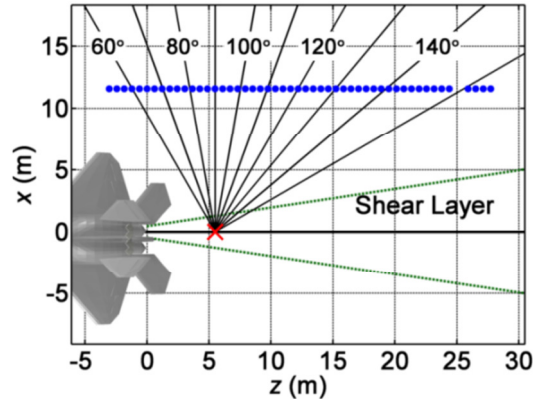


Figure 8. Measurement schematic involving ground-based linear array of Type-1 6.35 mm microphones for Holloman F-22 experiment.

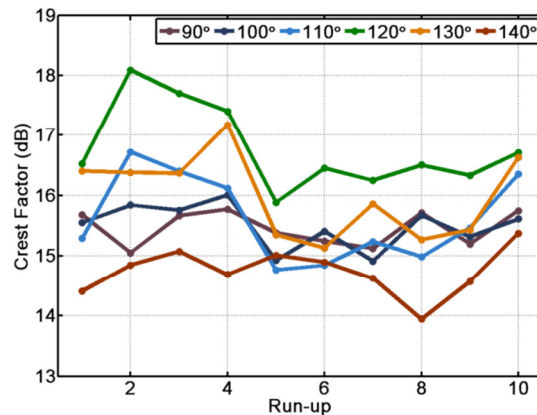


Figure 9. $CF_{99,999}$ for 10 static run-ups and several angles along the ground array in Figure 8.

Effect of Percentile Choice on Crest Factor

To examine the effect of percentile choice on the crest factor, the 150% F-35AA $CF_{99,9}$ and $CF_{99,99}$ were calculated and are displayed along with $CF_{99,999}$ and CF shown previously in Figure 7. The crest factor systematically increases with percentile, as expected. The directivity seems generally the

same, but there is a 2-2.5 dB increase in maximum crest factor with each decimal place increase in percentile.

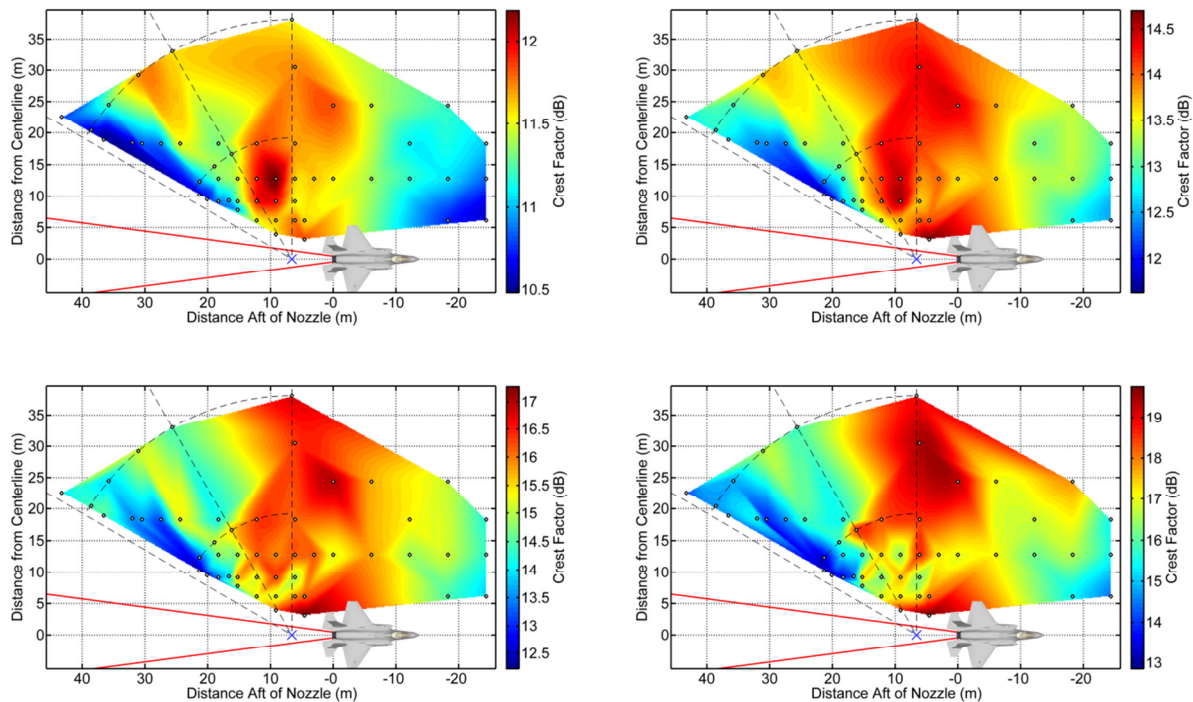


Figure 10. $CF_{99.9}$, $CF_{99.99}$, $CF_{99.999}$, and CF for the F-35AA at maximum afterburner

Impact of Peak Clipping

The previous analysis in Figure 10 has shown that the choice of percentile can have a significant impact on the crest factor in the waveform, approximately 2-3 dB per order of magnitude change. These percentile-based crest factors can be used to simulate the effect of clipping on level and statistics by setting clipping thresholds at these crest factor limits. This was done previously by Horne *et al.*⁸ for a small rocket motor firing. Figure 11 shows the simulated clipping for a 130% waveform segment at about (18,18) m downstream of the nozzle, using percentile-based crest factors for 90 (1 sample in 10), 99 (1 sample in 100, etc.), 99.9, 99.99, 99.999, and 100. The overall effect on the waveform probability density function and the one-third octave band spectrum are shown in Figure 12 and Figure 13, respectively. Artificially large tails are created by the clipping, more so on the positive side of the distribution, due to the positive skewness present in high-power jet noise waveforms. Despite this, however, the change in the one-third octave band sound pressure level (see Figure 13) is relatively small, with the exception of 90 percentile clipping.

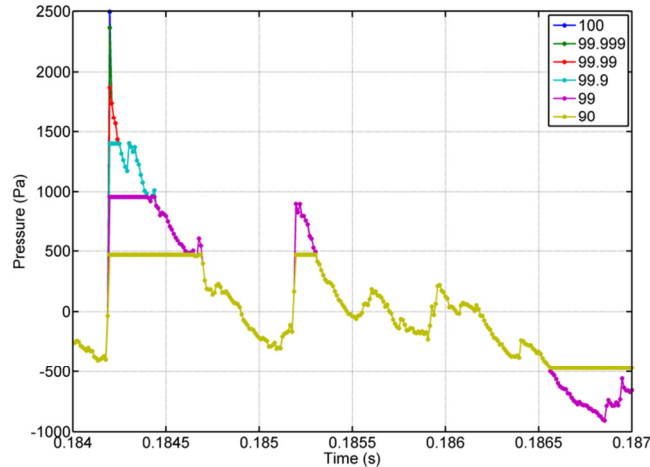


Figure 11. Afterburner waveform segments clipped at different percentiles beginning with 90.0.

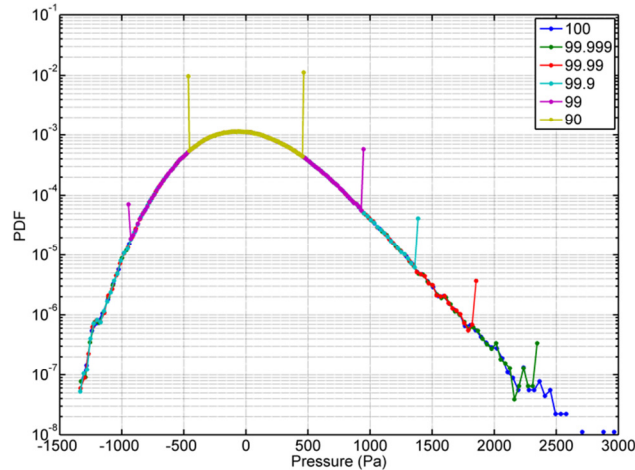


Figure 12. Probability density functions from afterburner waveform including clipping at different percentile levels.

Table 1 quantifies the errors in Figure 12 and Figure 13 using the OASPL (L_{rms}) and statistical measures, the skewness and the kurtosis, of both the time waveform and its derivative. The skewness is a measure of the distribution's asymmetry and the kurtosis is a measure of the distribution's relative peakedness. For a Gaussian distribution, the skewness is zero (the distribution is symmetric about its mean) and the kurtosis is equal to 3. The errors for 90 percentile are relatively large, which is not surprising given the dramatic impact on the waveform in Figure 11, but begin to drop rapidly as the simulated input range is increased. For 99th percentile clipping, the impact of the level within any one-third octave band within the bandwidth of interest (10-31.5 kHz) is less than 1 dB. However, the error in the positive skewness of the pressure waveform is relatively large as the positive peaks are substantially reduced.

Based on the results in Table 1 and Figure 13, it is clear that errors are small for both $CF_{99.99}$ and $CF_{99.999}$. Were it not for the derivative kurtosis error of 5%, it might be deemed acceptable to clip 1

sample in 10,000 (~1 sample every 0.1 s for a 96 kHz sampling rate). This is not a commonly used measure to characterize the noise field, however, and therefore a dynamic signal headroom based on $CF_{99,99}$ may be acceptable for many measurements. If detailed waveform analyses are required, $CF_{99,999}$ would be a better choice.

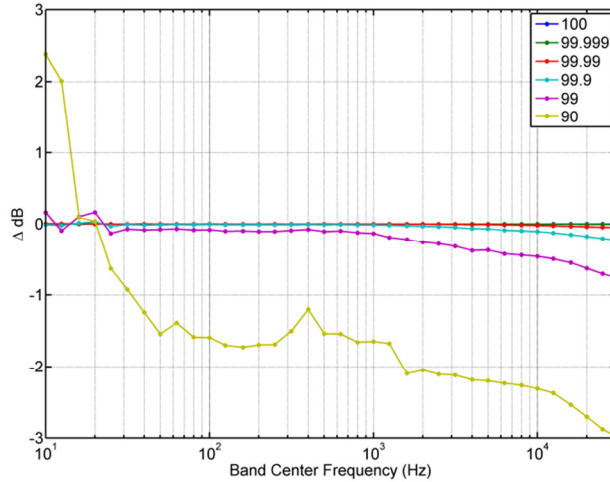


Figure 13. Effect of clipping at various percentiles on afterburner one-third octave band levels.

Table 1. Effect of percentile-based clipping on afterburner OASPL and statistics

Percentile	90	99	99.9	99.99	99.999	100
Δ OASPL (dB)	-1.7	-0.16	-0.022	-0.003	-0.0002	-----
$Sk\{p(t)\}$	0.0927	0.277	0.381	0.404	0.409	0.409
Error	77.4%	32.3%	7.06%	1.22%	0.12%	-----
$Sk\{\partial p/\partial t\}$	5.30	5.78	6.10	6.30	6.36	6.38
Error	16.9%	9.39%	4.35%	1.29%	0.24%	-----
$Ku\{p(t)\}$	1.89	2.91	3.31	3.45	3.48	3.49
Error	45.8%	16.4%	4.89%	1.10%	0.15%	-----
$Ku\{\partial p/\partial t\}$	52.0	64.4	74.8	82.7	86.5	87.4
Error	40.5%	26.3%	14.5%	5.4%	1.08%	-----

Summary

To summarize the findings:

- Crest factor generally increases as a function of engine power between 25% - 130%. Crest factor directivity at high engine powers is more toward the sideline than L_{rms} . A similar phenomenon has been seen with waveform skewness, which suggests a likely tie between crest factor, skewness and high-frequency energy. High-frequency noise radiation has a peak directivity farther upstream than low-frequency noise.
- Choice of percentile is critical part of definition of crest factor. Is it appropriate to define crest factor based off a single value in a 30 second waveform (1:3,000,000 for a ~100 kHz sampling rate)? This seems unnecessarily stringent and a percentile-based crest factor seems appropriate. Use of a $CF_{99,99}$ is perfectly sufficient to design a system in instances where only level-based measurements are required, but in instances where waveform analyses are desired, $CF_{99,999}$ (possible clipping of ~1 sample per second for 96 kHz sampling rate) is more appropriate. What does this mean in terms of crest factor?

Data acquisition system design and transducer selection based 15-17 dB headroom may result in clipping of 1 sample per every 0.1-1 second (assuming 96 kHz sampling), which has a very minimal impact on most measures of interest. However, where possible, allowance for at least a 20 dB crest factor in data acquisition system design and transducer selection is an appropriate recommendation based on current high-performance tactical engines.

Acknowledgments

This proceedings paper was prepared as part of an uninstalled jet engine measurement standard working group, funded by the U.S. Office of Naval Research (Joe Doychak, monitor), and supported by Richard McKinley of Air Force Research Laboratory and Allan Aubert of U.S. Naval Air Command. Distribution A: Approved for public release; distribution unlimited; 88ABW-2013-4806.

References

- ¹ S. A. McInerny, "Launch vehicle acoustics Part 2: Statistics of the time domain data," *J. Aircraft* **33**, 518-523 (1996).
- ² K. L. Gee, T. B. Neilsen, J. M. Downing, M. M. James, R. L. McKinley, R. C. McKinley, and A. T. Wall, "Near-field shock formation in noise propagation from a high-power jet aircraft," *J. Acoust. Soc. Am.* **133**, EL88-EL93 (2013).
- ³ K. L. Gee, T. B. Neilsen, M. B. Muhlestein, A. T. Wall, J. M. Downing, and M. M. James, "On the evolution of crackle in jet noise from high-performance engines, AIAA paper 2013-2190.
- ⁴ A. T. Wall, K. L. Gee, M. M. James, K. A. Bradley, S. A. McInerny, and T. B. Neilsen, "Near-field noise measurements of a high-performance military jet aircraft," *Noise Control Eng. J.* **60**, 421-434 (2012).
- ⁵ K. L. Gee, V. W. Sparrow, M. M. James, J. M. Downing, C. M. Hobbs, T. B. Gabrielson, and A. A. Atchley, "The role of nonlinear effects in the propagation of noise from high-power jet aircraft," *J. Acoust. Soc. Am.* **123**, 4082-4093 (2008).
- ⁶ K. L. Gee, V. W. Sparrow, M. M. James, J. M. Downing, C. M. Hobbs, T. B. Gabrielson, and A. A. Atchley, "Measurement and prediction of noise propagation from a high-power jet aircraft," *AIAA J.* **45**, 3003-3006 (2007).
- ⁷ R. H. Schlinker, S. A. Liljenberg, D. R. Polak, K. A. Post, C. T. Chipman, and A. M. Stern, "Supersonic jet noise source characteristics & propagation: Engine and model scale," AIAA Paper No. 2007-3623 (2007).
- ⁸ W. C. Horne, N. J. Burnside, J. Panda, and C. Brodell, "Measurements of unsteady pressures near the plume of a solid rocket motor," AIAA paper 2009-3323, May 2009.